

Solvent-modulation of the structure and dimensionality in lanthanoid-anilato coordination polymers

*Samia Benmansour**, *Irene Pérez Herráez*, *Christian Cerezo Navarrete*, *Gustavo López Martínez*, *Cristian Martínez-Hernández* and *Carlos J. Gómez García**

Supporting Information

Powder X-ray Diffraction analysis (PXRD)

The phase purity of all compounds except **2** was confirmed by comparing their experimental powder X-ray diffraction patterns with the simulated ones from the single crystal X-ray structure determination. For compound **2** we only obtained a few single crystals and could not perform a powder X-ray diffractogram. These diffratograms are displayed in figures S1-S5 for compounds **1**, **3-6**, respectively.

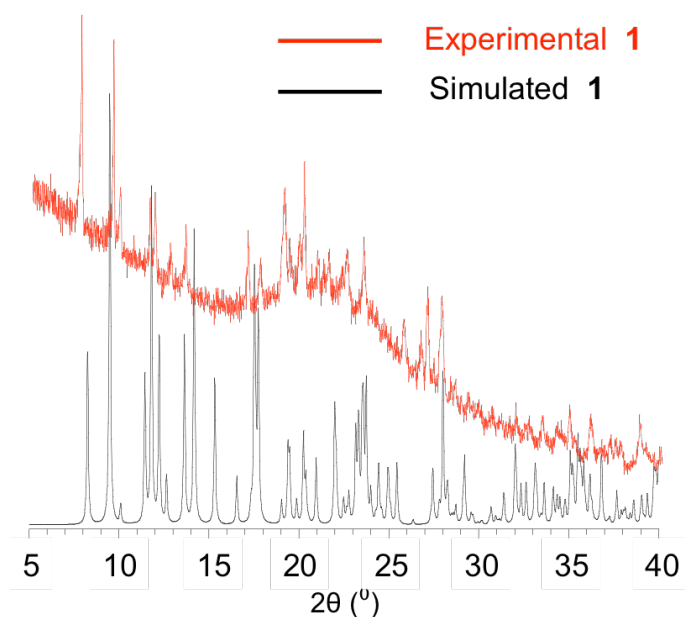


Figure S1. Experimental and simulated X-ray powder diffraction patterns for compound $[\text{Er}_2(\text{C}_6\text{O}_4\text{Cl}_2)_3(\text{H}_2\text{O})_6] \cdot 10\text{H}_2\text{O}$ (**1**).

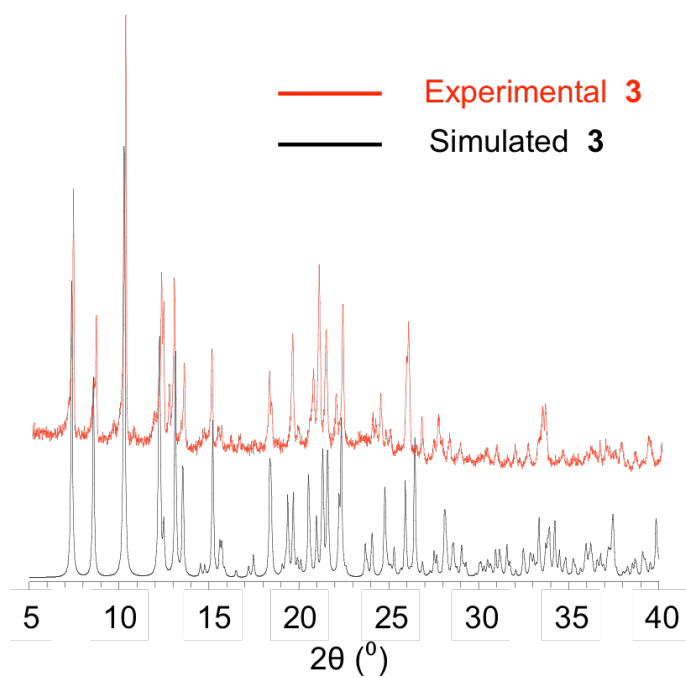


Figure S2. Experimental and simulated X-ray powder diffractograms for compound $[\text{Er}_2(\text{C}_6\text{O}_4\text{Cl}_2)_3(\text{DMSO})_4] \cdot 2\text{DMSO} \cdot 2\text{H}_2\text{O}$ (**3**).

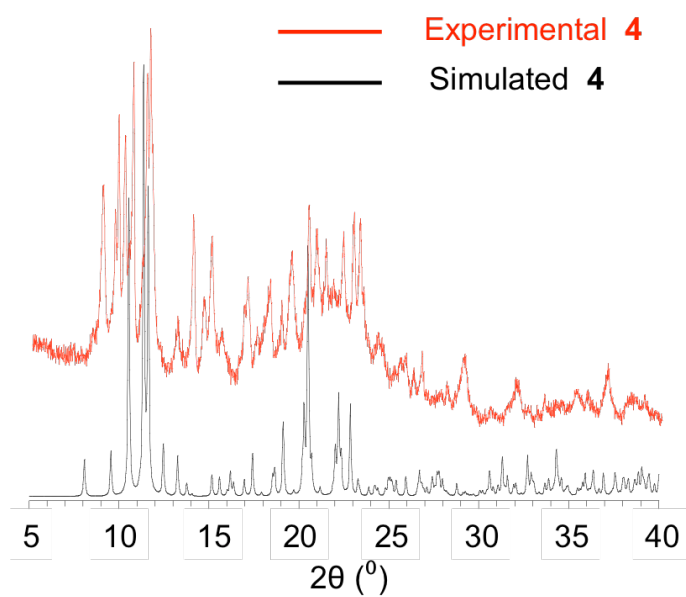


Figure S3. Experimental and simulated X-ray powder diffractograms for compound $[\text{Er}_2(\text{C}_6\text{O}_4\text{Cl}_2)_3(\text{DMF})_6]$ (**4**).

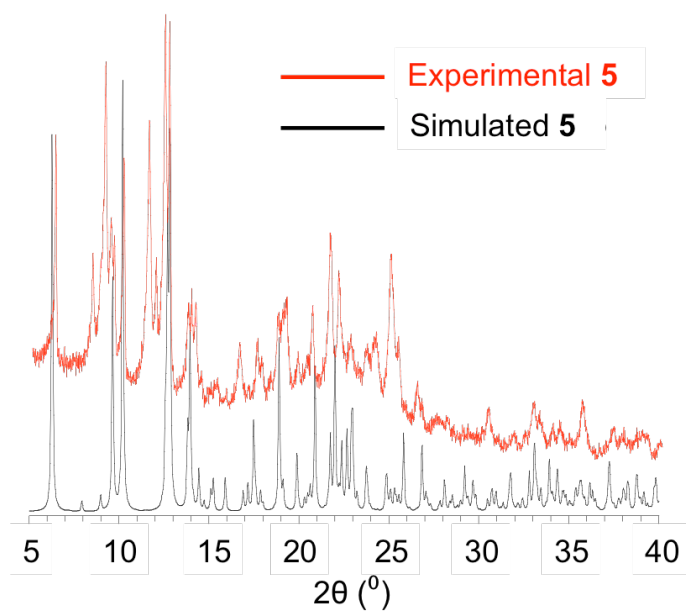


Figure S4. Experimental and simulated X-ray powder diffractograms for compound $[\text{Er}_2(\text{C}_6\text{O}_4\text{Cl}_2)_3(\text{DMA})_4]$ (**5**).

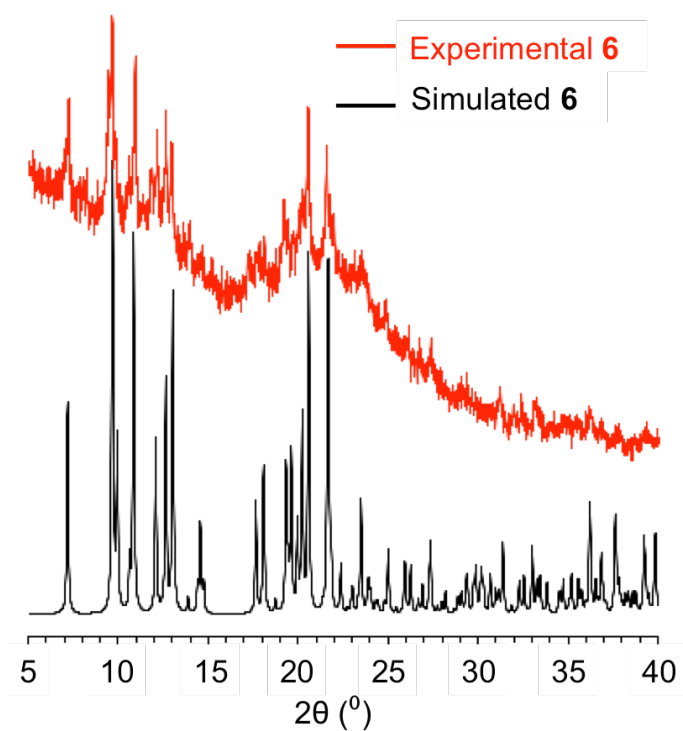


Figure S5. Experimental and simulated X-ray powder diffractograms for compound $[\text{Er}_2(\text{C}_6\text{O}_4\text{Cl}_2)_3(\text{HMPA})(\text{H}_2\text{O})_3] \cdot \text{H}_2\text{O}$ (**6**).

Table S1. Er-O bond distances (Å) for compounds [Er₂(C₆O₄Cl₂)₃(H₂O)₆] \cdot 10H₂O (1), [Er₂(C₆O₄Cl₂)₃(FMA)₆] \cdot 4FMA \cdot 2H₂O (2), [Er₂(C₆O₄Cl₂)₃(DMSO)₄] \cdot 2DMSO \cdot 2H₂O (3), [Er₂(C₆O₄Cl₂)₃(DMF)₆] (4), [Er₂(C₆O₄Cl₂)₃(DMA)₄] (5) and [Er₂(C₆O₄Cl₂)₃(HMPA)(H₂O)₃] \cdot H₂O (6).

Compound 1		Compound 2		Compound 3	
Atoms	dist. (Å)	Atoms	dist. (Å)	Atoms	dist. (Å)
Er1-O2	2.356(5)	Er1-O2	2.360(3)	Er1-O2	2.364(4)
Er1-O6 ^{#3}	2.440(6)	Er1-O3	2.416(3)	Er1-O6 ^{#4}	2.349(4)
Er1-O12	2.374(6)	Er1-O12	2.335(3)	Er1-O12	2.354(4)
Er1-O16 ^{#1}	2.394(6)	Er1-O13	2.381(3)	Er1-O16 ^{#6}	2.375(4)
Er1-O22	2.363(6)	Er1-O22	2.446(3)	Er1-O22	2.343(4)
Er1-O26 ^{#2}	2.422(5)	Er1-O23	2.368(3)	Er1-O26 ^{#5}	2.371(4)
Er1-O1W	2.319(6)	Er1-O1F	2.369(3)	Er1-O1D	2.294(5)
Er1-O2W	2.433(6)	Er1-O11F	2.327(3)	Er1-O11D	2.260(5)
Er1-O3W	2.441(6)	Er1-O21F	2.450(4)		
Ln-O _{an} ^a	2.392	Ln-O _{an} ^a	2.384	Ln-O _{an} ^a	2.359
Ln-O _{sol} ^b	2.398	Ln-O _{sol} ^b	2.382	Ln-O _{sol} ^b	2.277
Compound 4		Compound 5		Compound 5	
Atoms	dist. (Å)	Atoms	dist. (Å)	Atoms	dist. (Å)
Er1-O2	2.439(4)	Er1-O2	2.336(13)	Er2-O5	2.361(12)
Er1-O3	2.362(4)	Er1-O3	2.387(14)	Er2-O6	2.388(13)
Er1-O12	2.381(4)	Er1-O12	2.407(14)	Er2-O15 ^{#7}	2.396(14)
Er1-O13	2.423(4)	Er1-O13	2.336(12)	Er2-O16 ^{#7}	2.331(12)
Er1-O22	2.407(5)	Er1-O22	2.396(13)	Er2-O25 ^{#8}	2.357(13)
Er1-O23	2.412(4)	Er1-O23	2.331(14)	Er2-O26 ^{#8}	2.318(14)
Er1-O1D	2.337(4)	Er1-O1D	2.326(17)	Er2-O22D	2.232(16)
Er1-O11D	2.395(5)	Er1-O11D	2.220(15)	Er2-O32D	2.311(16)
Er1-O21D	2.401(4)	Ln-O _{an} ^a	2.366	Ln-O _{an} ^a	2.359
Ln-O _{an} ^a	2.404	Ln-O _{sol} ^b	2.273	Ln-O _{sol} ^b	2.272

Compound 6		Compound 6	
Atoms	dist. (Å)	Atoms	dist. (Å)
Er1-O2	2.365(9)	Er2-O5 ^{#10}	2.344(11)
Er1-O2 ^{#9}	2.365(9)	Er2-O5 ^{#11}	2.344(11)
Er1-O3	2.423(9)	Er2-O6 ^{#10}	2.409(11)
Er1-O3 ^{#9}	2.423(9)	Er2-O6 ^{#11}	2.409(11)
Er1-O12A	2.3286(14)	Er2-O16A	2.324(3)
Er1-O12B	2.3213(16)	Er2-O16B	2.325(3)
Er1-O1W	2.348(10)	Er2-O2W	2.332(10)
Er1-O1D	2.181(10)	Er2-O3W	2.327(10)
Ln-O _{an} ^a	2.371	Ln-O _{an} ^a	2.359
Ln-O _{sol} ^b	2.265	Ln-O _{sol} ^b	2.330

Symmetry transformations used to generate equivalent atoms:

#1 = -x, -y+1, -z+1; #2 = -x+1, -y+2, -z+1; #3 = -x, -y+2, -z; #4 = -x,-y,-z+2;

#5 = -x+1,-y+1,-z+1; #6 = -x,-y,-z+1; #7 = x-1,y,z-1; #8 = x,y,z-1; #9 = x,-y+1,z;

#10 = -x+3/2,-y+3/2,-z+1/2; #11 = -x+3/2,y-1/2,-z+1/2.

^aAverage Ln-O bond distance of the anilato oxygen atoms;

^bAverage Ln-O bond distance of the solvent oxygen atoms.

Table S2. Intermolecular interactions (in Å) shorter than the sum of the Van der Waals radii in compound $[\text{Er}_2(\text{C}_6\text{O}_4\text{Cl}_2)_3(\text{H}_2\text{O})_6] \cdot 10\text{H}_2\text{O}$ (**1**).

Atom 1	Atom 2	Sym. At. 1	Sym. At. 2	distance	Atom 1	Atom 2	Sym. At. 1	Sym. At. 2	distance
O1W	O11W	-x,1-y,1-z	-1+x,-1+y,1+z	2.667	O6	O22	-x,2-y,-z	-x,2-y,-z	2.874
O26	O2W	1-x,2-y,1-z	1-x,2-y,1-z	2.702	O2	O12	-x,2-y,-z	-x,2-y,-z	2.907
O2	O16	-x,2-y,-z	-x,2-y,-z	2.712	O14W	O15W	x,y,z	x,y,1+z	2.911
O6	O3W	-x,2-y,-z	-x,2-y,-z	2.742	O6	O11W	x,y,z	x,y,z	2.940
O26	O3W	1-x,2-y,1-z	1+x,y,z	2.769	Cl11	O16	x,y,z	-x,1-y,1-z	2.968
O26	O12	1-x,2-y,1-z	1-x,2-y,1-z	2.769	O2	Cl1	-x,1-y,1-z	-x,1-y,1-z	2.973
O13W	O14W	x,y,z	x,y,z	2.784	O26	Cl21	-x,1-y,1-z	-1+x,-1+y,z	2.975
O6	O1W	-x,2-y,-z	-x,2-y,-z	2.813	O12W	O13W	x,y,z	x,y,z	2.995
O1W	O14W	-x,1-y,1-z	-1+x,y,z	2.819	O2	O3W	-x,2-y,-z	-x,2-y,-z	3.019
O12	O3W	-x,1-y,1-z	x,-1+y,z	2.823	O14W	O14W	x,y,z	1-x,1-y,2-z	3.024
O22	O11W	x,y,z	x,y,z	2.825	O22	Cl21	-x,1-y,1-z	-x,1-y,1-z	3.028
O22	O2W	1-x,2-y,1-z	1-x,2-y,1-z	2.858	O6	Cl1	-x,1-y,1-z	x,-1+y,1+z	3.032
O2W	O13W	-x,1-y,1-z	-1+x,y,z	2.867	O12	Cl11	x,y,z	x,y,z	3.037
O12W	O15W	x,y,z	x,y,1+z	2.872	Cl11	O22	-x,1-y,1-z	x,-1+y,z	3.176

Table S3. Intermolecular interactions (in Å) shorter than the sum of the Van der Waals radii in compound $[\text{Er}_2(\text{C}_6\text{O}_4\text{Cl}_2)_3(\text{FMA})_6] \cdot 4\text{FMA} \cdot 2\text{H}_2\text{O}$ (**2**).

Atom 1	Atom 2	Sym. At. 1	Sym. At. 2	distance	Atom 1	Atom 2	Sym. At. 1	Sym. At. 2	distance
O22	O21F	1-x,1-y,1-z	1-x,1-y,1-z	2.660	Cl11	O100	x,y,z	-1+x,y,z	2.954
O2	O13	1-x,1-y,-z	1-x,1-y,-z	2.682	O13	Cl11	x,y,z	-x,1-y,-z	2.957
O3	O23	1-x,1-y,-z	1-x,1-y,-z	2.726	O22	Cl21	x,y,z	x,y,z	2.978
O22	O11F	1-x,1-y,1-z	1-x,1-y,1-z	2.727	N11F	O23	x,y,z	1-x,-1/2+y,1/2-z	2.982
O3	O1F	1-x,1-y,-z	1-x,1-y,-z	2.747	O200	N200	x,y,z	-x,1-y,1-z	2.991
O22	O12	1-x,1-y,1-z	1-x,1-y,1-z	2.800	N21F	O1W	-x,1-y,-z	-x,-1/2+y,1/2-z	2.992
O2	O21F	1-x,1-y,-z	1-x,1-y,-z	2.805	O2	Cl1	x,y,z	x,y,z	3.006
O3	N11F	x,y,z	x,y,z	2.817	O3	Cl1	x,y,z	1-x,1-y,-z	3.021
O200	O1W	x,y,z	x,y,z	2.850	O12	Cl11	x,y,z	x,y,z	3.031
O2	O23	1-x,1-y,-z	1-x,1-y,-z	2.932	N1F	O100	-x,1-y,-z	1-x,1/2+y,1/2-z	3.043
O100	N200	x,y,z	1+x,y,z	2.944	O23	Cl21	x,y,z	1-x,1-y,1-z	3.055

Table S4. Intermolecular interactions (in Å) shorter than the sum of the Van der Waals radii in compound [Er₂(C₆O₄Cl₂)₃(DMSO)₄]·2DMSO·2H₂O (**3**).

Atom 1	Atom 2	Sym. At. 1	Sym. At. 2	distance	Atom 1	Atom 2	Sym. At. 1	Sym. At. 2	distance
O6	O16	x,y,z	x,y,1+z	2.819	O2	Cl1	-x,-y,1-z	-x,-y,1-z	3.006
O100	O1W	x,y,z	x,y,z	2.859	Cl11	O16	x,y,z	x,y,z	3.011
O6	O12	x,y,z	-x,-y,2-z	2.864	O6	Cl1	x,y,-1+z	x,y,-1+z	3.018
O26	O1D	x,y,z	1-x,1-y,1-z	2.894	O22	Cl21	-x,-y,1-z	-x,-y,1-z	3.020
O2	O1D	-x,-y,2-z	-x,-y,2-z	2.894	O12	Cl11	x,y,z	x,y,z	3.027
O26	O2	x,y,z	1-x,1-y,1-z	2.907	O22	O12	1-x,1-y,1-z	1-x,1-y,1-z	3.035
O26	O11D	x,y,z	1-x,1-y,1-z	2.933	S1D	O26	x,y,z	1-x,1-y,1-z	3.112
O2	O11D	-x,-y,2-z	-x,-y,2-z	2.978	O26	S1D'	x,y,z	1-x,1-y,1-z	3.193
O26	Cl21	-1+x,-1+y,z	-1+x,-1+y,z	3.001	O12	S11D	-x,-y,1-z	-1+x,y,z	3.261

AC susceptibility measurements

The AC susceptibility measurements do not show any out of phase signal in compounds 1 and 3-6 (Figures S6-S10).

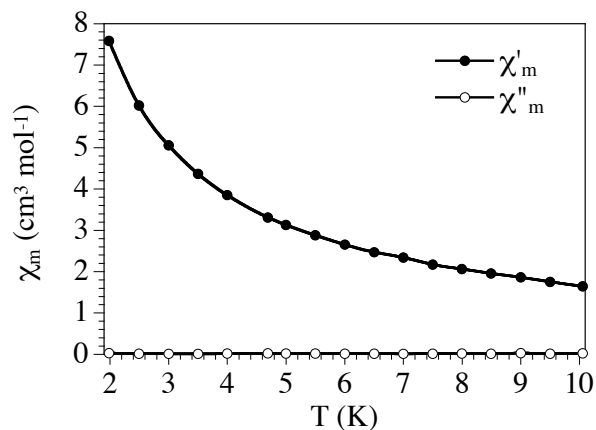


Figure S6. Thermal variation of the in phase (χ'_m) and out of phase (χ''_m) susceptibilities of compound $[\text{Er}_2(\text{C}_6\text{O}_4\text{Cl}_2)_3(\text{H}_2\text{O})_6] \cdot 10\text{H}_2\text{O}$ (**1**) in the low temperature region.

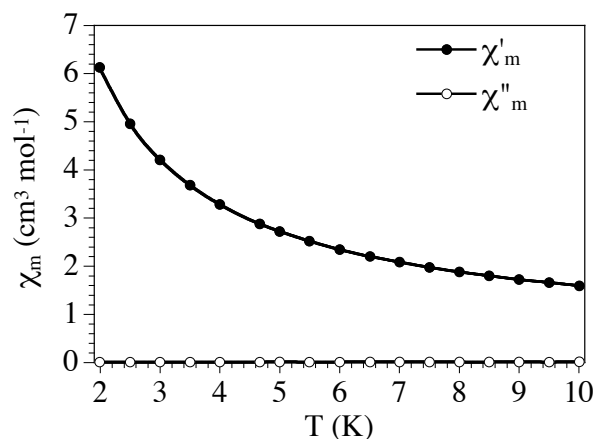


Figure S7. Thermal variation of the in phase (χ'_m) and out of phase (χ''_m) susceptibilities of compound $[\text{Er}_2(\text{C}_6\text{O}_4\text{Cl}_2)_3(\text{DMSO})_4] \cdot 2\text{DMSO} \cdot 2\text{H}_2\text{O}$ (**3**) in the low temperature region.

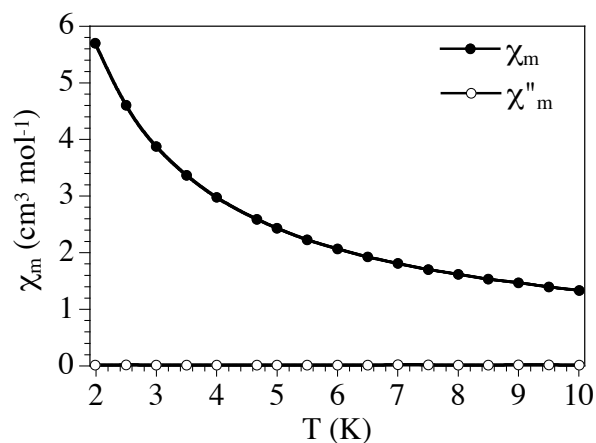


Figure S8. Thermal variation of the in phase (χ_m') and out of phase (χ_m'') susceptibilities of compound $[\text{Er}_2(\text{C}_6\text{O}_4\text{Cl}_2)_3(\text{DMF})_6]$ (**4**) in the low temperature region.

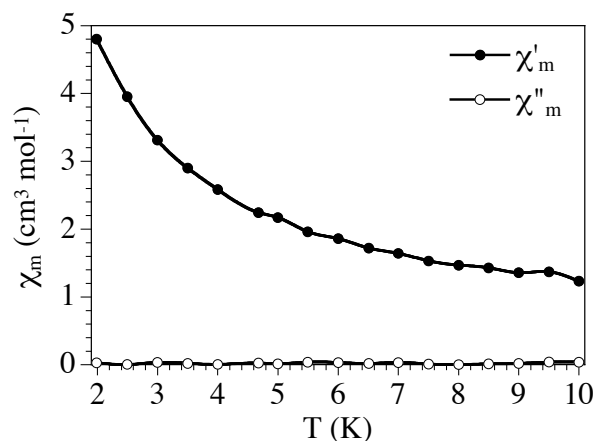


Figure S9. Thermal variation of the in phase (χ_m') and out of phase (χ_m'') susceptibilities of compound $[\text{Er}_2(\text{C}_6\text{O}_4\text{Cl}_2)_3(\text{DMA})_4]$ (**5**) in the low temperature region.

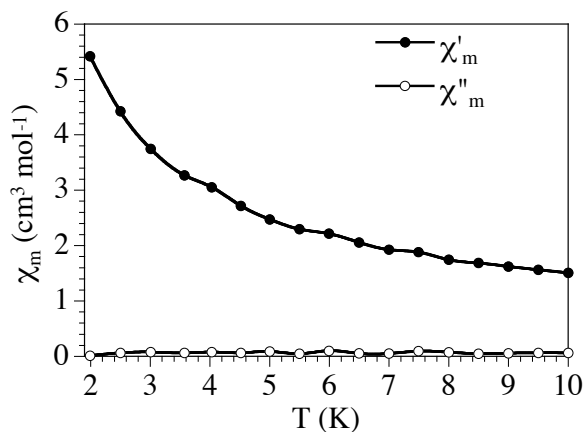


Figure S10. Thermal variation of the in phase (χ_m') and out of phase (χ_m'') susceptibilities of compound $[\text{Er}_2(\text{C}_6\text{O}_4\text{Cl}_2)_3(\text{HMPA})(\text{H}_2\text{O})_3] \cdot \text{H}_2\text{O}$ (**6**) in the low temperature region.

IR spectra

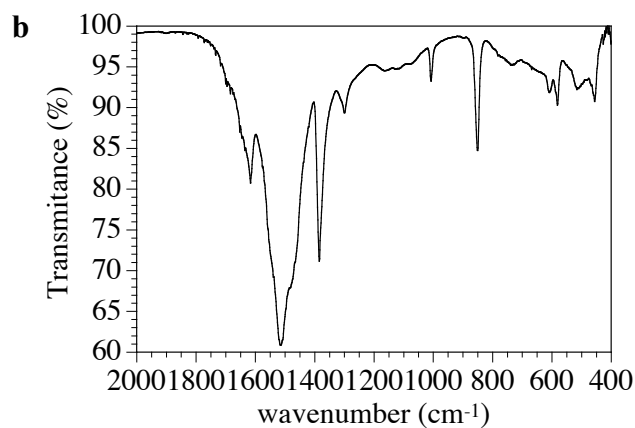
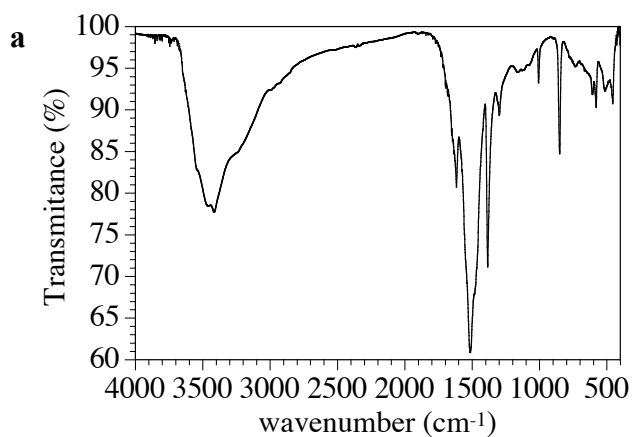


Figure S11. IR spectrum of compound $[\text{Er}_2(\text{C}_6\text{O}_4\text{Cl}_2)_3(\text{H}_2\text{O})_6] \cdot 10\text{H}_2\text{O}$ (**1**) in (a) the 4000-400 cm^{-1} and (b) 2000-400 cm^{-1} ranges.

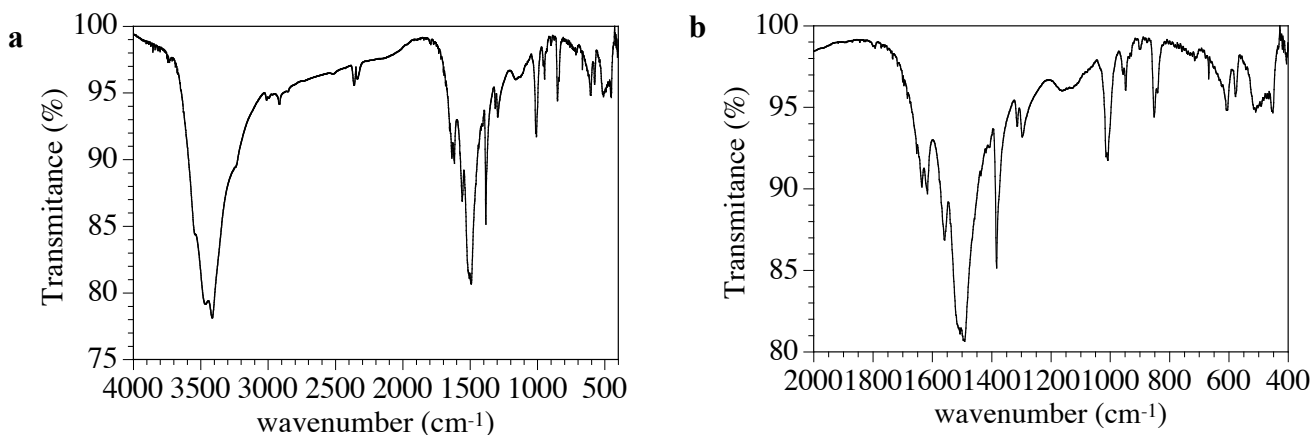


Figure S12. IR spectrum of compound $[\text{Er}_2(\text{C}_6\text{O}_4\text{Cl}_2)_3(\text{DMSO})_4] \cdot 2\text{DMSO} \cdot 2\text{H}_2\text{O}$ (**3**) in (a) the 4000-400 cm^{-1} and (b) 2000-400 cm^{-1} ranges.

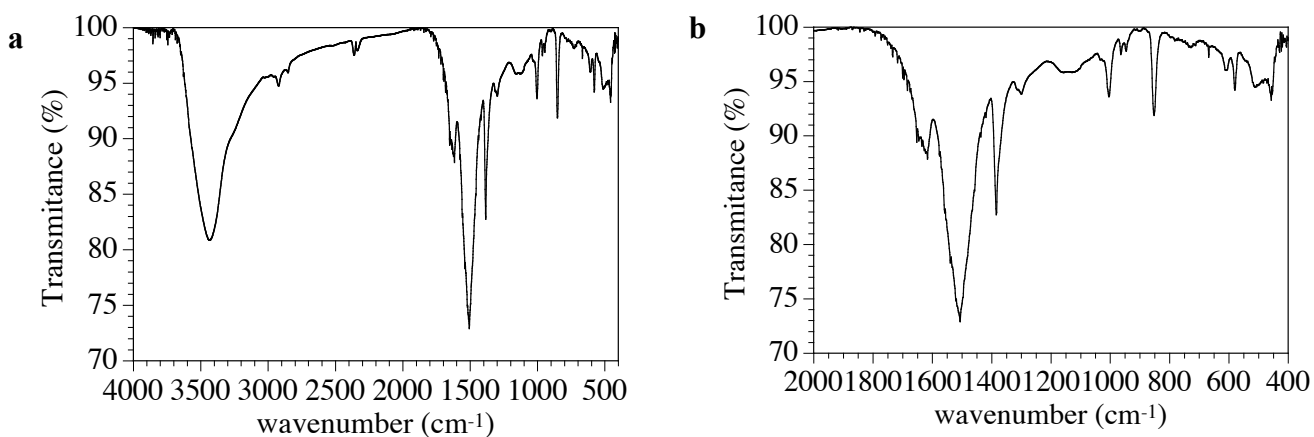


Figure S13. IR spectrum of compound $[\text{Er}_2(\text{C}_6\text{O}_4\text{Cl}_2)_3(\text{DMF})_6]$ (**4**) in (a) the 4000-400 cm^{-1} and (b) 2000-400 cm^{-1} ranges.

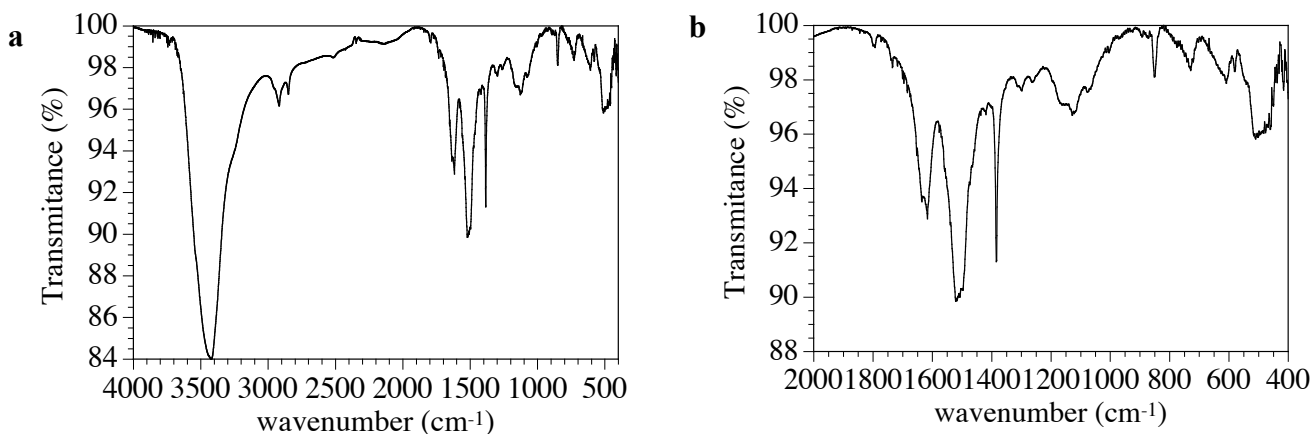


Figure S14. IR spectrum of compound $[\text{Er}_2(\text{C}_6\text{O}_4\text{Cl}_2)_3(\text{DMA})_4]$ (**5**) in (a) the 4000-400 cm^{-1} and (b) 2000-400 cm^{-1} ranges.

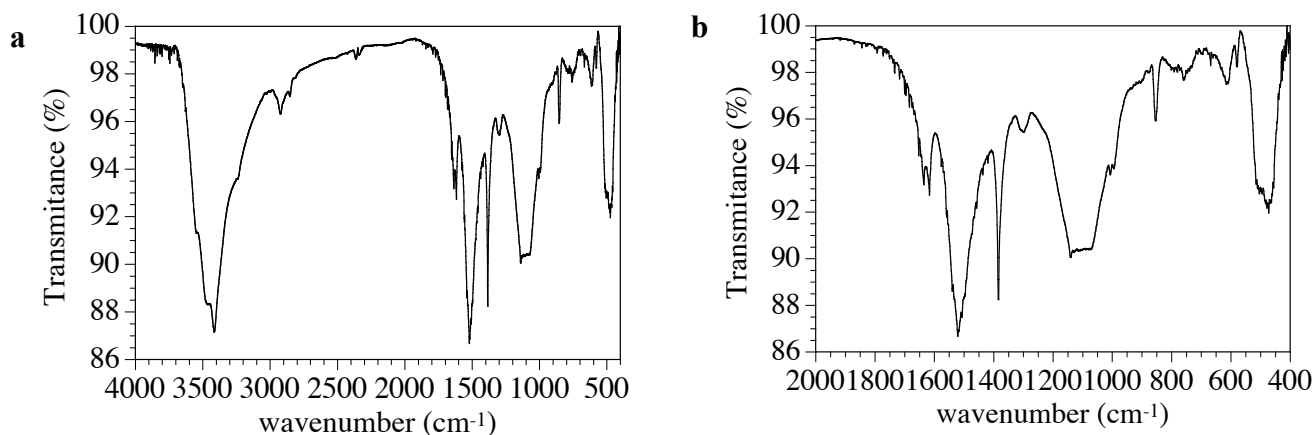


Figure S15. IR spectrum of compound $[\text{Er}_2(\text{C}_6\text{O}_4\text{Cl}_2)_3(\text{HMPA})(\text{H}_2\text{O})_3] \cdot \text{H}_2\text{O}$ (**6**) in (a) the 4000-400 cm^{-1} and (b) 2000-400 cm^{-1} ranges.

Table S5. Main IR bands and their assignment in compounds $[\text{Er}_2(\text{C}_6\text{O}_4\text{Cl}_2)_3(\text{H}_2\text{O})_6] \cdot 10\text{H}_2\text{O}$ (**1**), $[\text{Er}_2(\text{C}_6\text{O}_4\text{Cl}_2)_3(\text{DMSO})_4] \cdot 2\text{DMSO} \cdot 2\text{H}_2\text{O}$ (**3**), $[\text{Er}_2(\text{C}_6\text{O}_4\text{Cl}_2)_3(\text{DMF})_6]$ (**4**), $[\text{Er}_2(\text{C}_6\text{O}_4\text{Cl}_2)_3(\text{DMA})_4]$ (**5**) and $[\text{Er}_2(\text{C}_6\text{O}_4\text{Cl}_2)_3(\text{HMPA})(\text{H}_2\text{O})_3] \cdot \text{H}_2\text{O}$ (**6**).

	1 (H_2O)	3 (DMSO)	4 (DMF)	5 (DMA)	6 (HMPA)
$\nu(\text{C}=\text{O})$	1617	1617	1617	1617	1617
$\nu(\text{C}=\text{C}) + \nu(\text{C}-\text{O})$	1515	1491	1506	1521	1521
$\nu(\text{C}-\text{C}) + \nu(\text{C}-\text{O})$	1385	1384	1385	1384	1384
$\delta(\text{C}-\text{X})$	851	852	853	851	854
$\rho(\text{C}-\text{X})$	581	578	580	581	580

Table S6. IR bands corresponding to the different solvents present in compounds $[\text{Er}_2(\text{C}_6\text{O}_4\text{Cl}_2)_3(\text{H}_2\text{O})_6] \cdot 10\text{H}_2\text{O}$ (**1**), $[\text{Er}_2(\text{C}_6\text{O}_4\text{Cl}_2)_3(\text{DMSO})_4] \cdot 2\text{DMSO} \cdot 2\text{H}_2\text{O}$ (**3**), $[\text{Er}_2(\text{C}_6\text{O}_4\text{Cl}_2)_3(\text{DMF})_6]$ (**4**), $[\text{Er}_2(\text{C}_6\text{O}_4\text{Cl}_2)_3(\text{DMA})_4]$ (**5**) and $[\text{Er}_2(\text{C}_6\text{O}_4\text{Cl}_2)_3(\text{HMPA})(\text{H}_2\text{O})_3] \cdot \text{H}_2\text{O}$ (**6**).

	1 (H_2O)	3 (DMSO)	4 (DMF)	5 (DMA)	6 (HMPA)
$\nu(\text{C}-\text{H})$	-	2916 2858	2922 2857	2918 2850	2923 2857
$\nu(\text{C}=\text{O})$	-	-	1617*	1617*	-

$\nu(\text{S=O})$	-	1008	-	-	-
$\rho(\text{C-S})$	-	948	-	-	-
$\nu(\text{O-H})$	3415	-	-	-	-
$\delta(\text{H-O-H})$	1617*	-	-	-	-

*overlapping with the corresponding $\nu(\text{C=O})$ band from the anilato ligand.

Shape analysis of the coordination geometries

The analysis with the program SHAPE¹ of the coordination geometries of the Er ions in the six compounds is summarized in tables S7 and S8.

Table S7. SHAPE values for the 13 possible coordination geometries found for coordination number nine² in compounds [Er₂(C₆O₄Cl₂)₃(H₂O)₆]·10H₂O (**1**), [Er₂(C₆O₄Cl₂)₃(FMA)₆]·4FMA·2H₂O (**2**) and [Er₂(C₆O₄Cl₂)₃(DMF)₆] (**4**).

Geometry	symmetry	1	2	4
EP-9	D _{9h}	35.635	37.024	37.487
OPY-9	C _{8v}	21.818	22.831	22.093
HBPY-9	D _{7h}	20.383	19.548	20.018
JTC-9	C _{3v}	15.990	15.298	16.510
JCCU-9	C _{4v}	11.196	9.427	9.788
CCU-9	C _{4v}	9.987	8.267	8.544
JCSAPR-9	C _{4v}	1.590	1.389	1.303
CSAPR-9	C _{4v}	0.558	0.442	0.282
JTCTPR-9	D _{3h}	1.930	2.200	2.634
TCTPR-9	D _{3h}	0.551	0.718	0.718
JTDIC-9	C _{3v}	13.149	12.02	11.910
HH-9	C _{2v}	12.272	12.039	12.513
MFF-9	C _s	1.146	0.822	0.866

EP-9 = Enneagon; OPY-9 = Octagonal pyramid; HBPY-9 = Heptagonal bipyramid; JTC-9 = Triangular cupola (J3) = trivacant cuboctahedron; JCCU-9 = Capped cube (Elongated square pyramid, J8); CCU-9 = Capped cube; JCSAPR-9 = Capped square antiprism (Gyroelongated square pyramid J10); CSAPR-9 = Capped square antiprism; JTCTPR-9 = Tricapped trigonal prism (J51); TCTPR-9 = Tricapped trigonal prism; JTDIC-9 = Tridiminished icosahedron (J63); HH-9 = Hula-hoop; MFF-9 = Muffin. The minima values are indicated in bold.

Table S8. SHAPE values for the 13 possible coordination geometries found for coordination numbers eight³ in compounds $[\text{Er}_2(\text{C}_6\text{O}_4\text{Cl}_2)_3(\text{DMSO})_4] \cdot 2\text{DMSO} \cdot 2\text{H}_2\text{O}$ (**3**), $[\text{Er}_2(\text{C}_6\text{O}_4\text{Cl}_2)_3(\text{DMA})_4] \cdot 5\text{H}_2\text{O}$ (**5**) and $[\text{Er}_2(\text{C}_6\text{O}_4\text{Cl}_2)_3(\text{HMPA})(\text{H}_2\text{O})_3] \cdot \text{H}_2\text{O}$ (**6**).

Geometry	symmetry	3	5-Er1	5-Er2	6-Er1	6-Er2
OP-8	D _{8h}	30.394	31.089	30.975	29.996	31.318
HPY-8	C _{7v}	23.430	21.448	21.964	23.182	22.549
HBPY-8	D _{6h}	15.038	14.435	14.703	16.170	15.653
CU-8	O _h	11.285	8.942	9.474	12.723	13.637
SAPR-8	D _{4d}	1.603	1.325	1.531	2.504	3.666
TDD-8	D _{2d}	1.126	1.139	1.153	2.071	2.698
JGBF-8	D _{2d}	12.921	14.639	14.188	13.613	12.634
JETBPY-8	D _{3h}	28.808	28.371	28.131	26.962	26.046
JBTP-8	C _{2v}	2.246	1.942	1.981	1.643	2.027
BTTP-8	C _{2v}	1.813	1.611	1.557	1.351	1.472
JSD-8	D _{2d}	2.929	3.543	3.578	3.778	4.317
TT-8	T _d	12.034	9.610	10.204	13.407	14.298
ETBPY-8	D _{3h}	24.079	24.18	24.189	24.401	22.974

OP-8 = Octagon; HPY-8 = Heptagonal pyramid; HBPY-8 = Hexagonal bipyramid; CU-8 = Cube; SAPR-8 = Square antiprism; TDD-8 = Triangular dodecahedron; JGBF-8 = Johnson-Gyrobifastigium (J26); JETBPY-8 = Johnson-Elongated triangular bipyramid (J14); JBTP-8 = Johnson-Biaugmented trigonal prism (J50); BTTP-8 = Biaugmented trigonal prism, JSD-8 = Snub disphenoid (J84); TT-8 = Triakis tetrahedron; ETBPY-8 = Elongated trigonal bipyramid. The minima values are indicated in bold.

Ortep plots of the asymmetric units of compounds 1-6

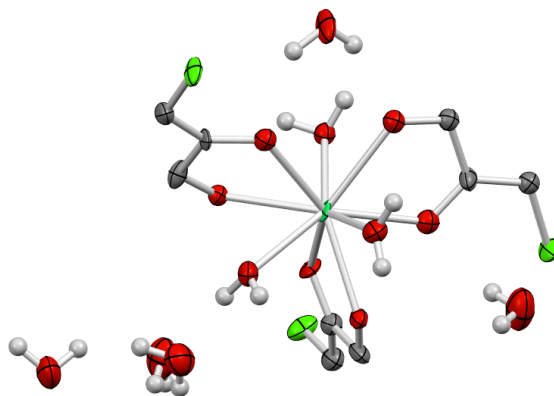


Figure S16. ORTEP plot (ellipsoids at 80 % probability) of the asymmetric unit of compound $[\text{Er}_2(\text{C}_6\text{O}_4\text{Cl}_2)_3(\text{H}_2\text{O})_6] \cdot 10\text{H}_2\text{O}$ (**1**).

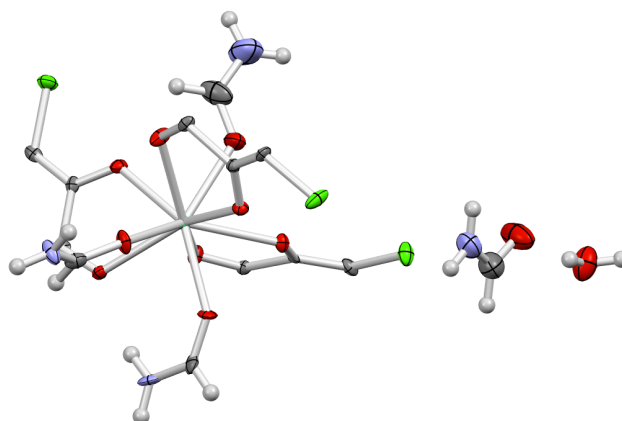


Figure S17. ORTEP plot (ellipsoids at 60 % probability) of the asymmetric unit of compound $[\text{Er}_2(\text{C}_6\text{O}_4\text{Cl}_2)_3(\text{FMA})_6] \cdot 4\text{FMA} \cdot 2\text{H}_2\text{O}$ (**2**).

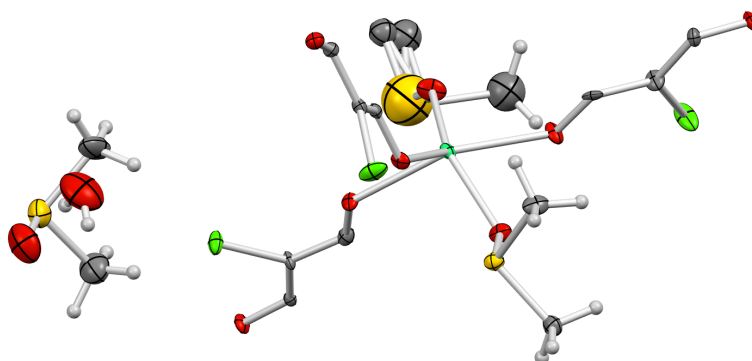


Figure S18. ORTEP plot (ellipsoids at 50 % probability) of the asymmetric unit of compound $[\text{Er}_2(\text{C}_6\text{O}_4\text{Cl}_2)_3(\text{DMSO})_4] \cdot 2\text{DMSO} \cdot 2\text{H}_2\text{O}$ (**3**).

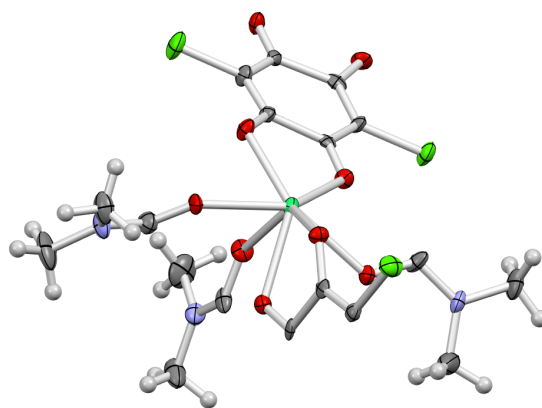


Figure S19. ORTEP plot (ellipsoids at 50 % probability) of the asymmetric unit of compound $[\text{Er}_2(\text{C}_6\text{O}_4\text{Cl}_2)_3(\text{DMF})_6]$ (**4**).

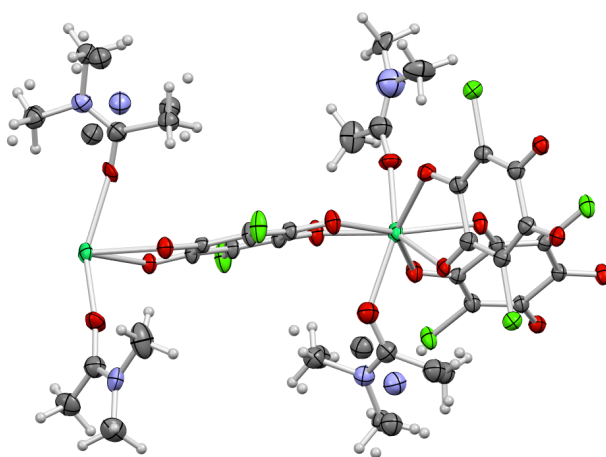


Figure S20. ORTEP plot (ellipsoids at 30 % probability) of the asymmetric unit of compound $[\text{Er}_2(\text{C}_6\text{O}_4\text{Cl}_2)_3(\text{DMA})_4]$ (**5**).

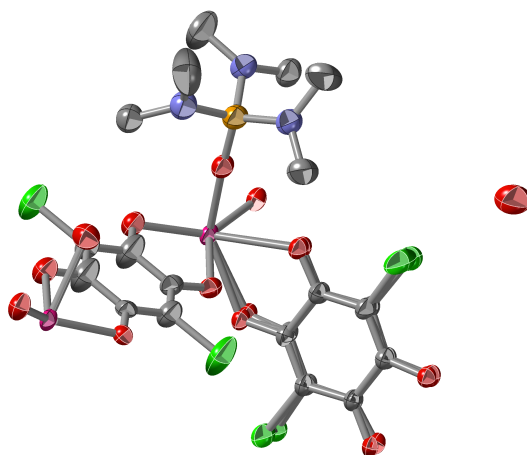
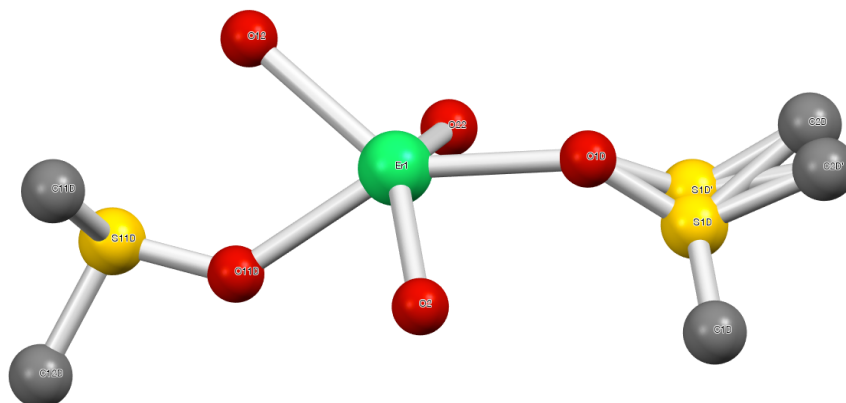


Figure S21. ORTEP plot (ellipsoids at 90 % probability) of the asymmetric unit of compound $[\text{Er}_2(\text{C}_6\text{O}_4\text{Cl}_2)_3(\text{HMPA})(\text{H}_2\text{O})_3] \cdot \text{H}_2\text{O}$ (**6**).

Single crystal X-ray structure analysis of the disorder in the solvent molecules.

$[\text{Er}_2(\text{C}_6\text{O}_4\text{Cl}_2)_3(\text{DMSO})_4]\cdot 2\text{DMSO}\cdot 2\text{H}_2\text{O}$ (**3**). In this compound one of the two coordinated DMSO molecules appear with the S atom disordered in two very close positions (S1D and S1D') with equal occupancies (0.5 each). There is also a disorder in one of the two C atoms (C2D and C2D') connected to the S atoms. These carbon atoms were refined with different occupancy factors (0.75 or C2D and 0.25 for C2D', see figure S22).



$[\text{Er}_2(\text{C}_6\text{O}_4\text{Cl}_2)_3(\text{HMPA})(\text{H}_2\text{O})_3] \cdot \text{H}_2\text{O}$ (**6**). In this compound the coordinated hexamethylphosphoramide molecule appears with a disorder of the three $-\text{N}(\text{CH}_3)_2$ groups delocalized over two positions related through a mirror plane that passes through the P, O atoms of the molecule. These two positions present, therefore, occupancy factors of 0.5 each, see figure S24).

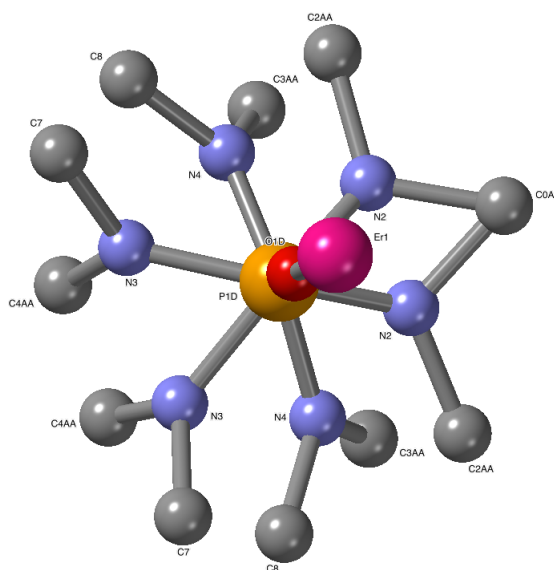


Figure S24. Fragment of the asymmetric unit of compound $[\text{Er}_2(\text{C}_6\text{O}_4\text{Cl}_2)_3(\text{HMPA})(\text{H}_2\text{O})_3] \cdot \text{H}_2\text{O}$ (**6**) showing the disorder of the coordinated hexamethylphosphoramide molecule.

References

- 1- Lluell, M.; Casanova, D.; Cirera, J.; Bofill, J. M.; Alemany, P.; Alvarez, S.; Pinsky, M.; Avnir, D. SHAPE, version 2.3, University of Barcelona, Barcelona, Spain, and Hebrew University of Jerusalem, Jerusalem, Israel, **2013**.
- 2- Ruiz-Martínez, A.; Casanova, D.; Alvarez, S. Polyhedral Structures with an Odd Number of Vertices: Nine-Coordinate Metal Compounds. *Chem. Eur. J.* **2008**, *14*, 1291-1303.
- 3- Casanova, D.; Lluell, M.; Alemany, P.; Alvarez, S. The Rich Stereochemistry of Eight-Vertex Polyhedra: A Continuous Shape Measures Study. *Chem. Eur. J.* **2005**, *11*, 1479-1494.